ACS APPLIED MATERIALS & INTERFACES

Forum Article

www.acsami.org

Micropatterned Hydrogel Surface with High-Aspect-Ratio Features for Cell Guidance and Tissue Growth

Yuhang Hu,*[,†,‡] Jin-Oh You,[†,§] and Joanna Aizenberg[†,⊥,∥,#]

[†]John A. Paulson School of Engineering and Applied Sciences, Harvard University, Cambridge, Massachusetts 02138, United States

[‡]Department of Mechanical Science and Engineering, University of Illinois at Urbana−Champaign, Urbana, Illinois 61801, United States

[§]Department of Engineering Chemistry, Chungbuk National University, Cheongju 362-763, Republic of Korea

[⊥]Wyss Institute for Biologically Inspired Engineering, Harvard University, Cambridge, Massachusetts 02138, United States

[∥]Department of Chemistry and Chemical Biology, Harvard University, Cambridge, Massachusetts 02138, United States

[#]Kavli Institute for Bionano Science and Technology, Harvard University, Cambridge, Massachusetts 02138, United States

Supporting Information

ABSTRACT: Surface topography has been introduced as a new tool to coordinate cell selection, growth, morphology, and differentiation. The materials explored so far for making such structural surfaces are mostly rigid and impermeable. Hydrogel, on the other hand, was proved a better synthetic media for cell culture because of its biocompatibility, softness, and high permeability. Herein, we fabricated a poly(2-hydroxyethyl methacrylate) (pHEMA) hydrogel substrate with high-aspect-ratio surface microfeatures. Such structural surface could effectively guide the orientation and shape of human mesenchymal stem cells (HMSCs). Notably, on the flat hydrogel surface, cells rounded up, whereas on the microplate patterned hydrogel surface, cells elongated and aligned along the direction parallel to the plates. The microplates were 2 μm thick, 20 μm tall, and 10−50 μm wide. The interplate spacing was 5−15 μm, and the intercolumn spacing was 5 μm. The elongation of cell body was more pronounced on the patterns with narrower interplate spacing and wider plates. The cells behaved like soft solid. The competition between surface energy and elastic energy defined the shape of the cells on the structured surfaces. The soft permeable hydrogel scaffold with surface structures was also demonstrated as being viable for long-term cell culture, and could be used to generate interconnected tissues with finely tuned cell morphology and alignment across a few centimeter sizes.

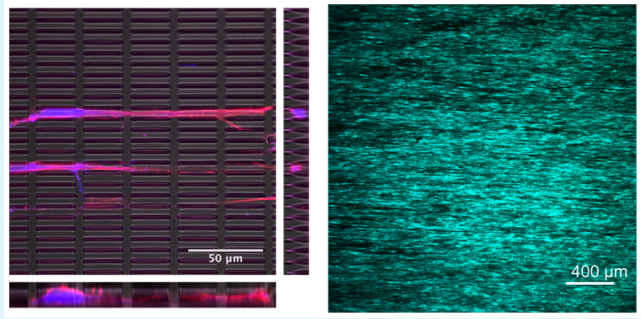

KEYWORDS: *cell alignment, cell adhesion, hydrogel, structured surface, human mesenchymal stem cell, tissue scaffold*

1. INTRODUCTION

Cellular alignment of native tissues plays a crucial role in many biological functions.[1−4] The ability to control cell shape and to engineer tissues with precisely controlled morphology holds great potential in many biomedical applications including regenerative medicine,[5] tissue regeneration and repair,[6,7] drug screening,[7,8] development of biosensors,[9] and elucidation of cell−cell and cell−matrix interactions.[10,11]

Cells constantly sense and respond to a variety of signals from the environment over a wide range of length scales.[12] The interaction between cells and the biochemical and biophysical cues imposed by the extracellular environment plays a central role in mediating many cell properties and functions. A precise control of cell alignment and organization in vitro relies on a robust micro/nano-fabrication technique to construct a synthetic extracellular environment mimicking the native biological environment. To address this need, one popular technique is to fabricate and use a culture substrate with microscopic features that impose a defined cell adhesion pattern.[13−15] This technique has been used to study the influence of cell shape on its architecture,[16] migration,[17,18] differentiation,[19] and growth.[20] Although the micropatterning technique has shown success in controlling single cell shape and adhesion location, it is not applicable to generate continuous tissue due to the existence of the separations between adhesion patches. Another widely explored technique is to fabricate substrate with nano/micro-topographical patterns, on which the cells elongate and align on the structured surface through a phenomenon called contact

Special Issue: Interfaces for Mechanobiology and Mechanochemistry: From 2-D to 3-D Platforms

Received: December 16, 2015
Accepted: April 5, 2016
Published: April 18, 2016

DOI: 10.1021/acsami.5b12268
ACS Appl. Mater. Interfaces 2016, 8, 21939−21945

guidance.[21,22] The elongated cell body can induce directional migration, which can facilitate wound healing[23] and alter gene expression.[24] However, to induce effective mechanotransductive cues, the size of the topographical features for most cells is in the hundreds of nanometers to a few micrometers range, which limits the choice of materials.

The materials explored so far[21−38] are mostly rigid and impermeable, which are hard to be used in long-term cell culture and tissue transplantation. Noncompliant materials can cause localized inflammation in the dynamic in vivo environment.[39] Besides, cells in the body reside in close proximity to blood vessels that supply tissues with nutrients and oxygen and remove waste products and carbon dioxide. It is important to engineer an environment that can perform a similar function. To meet these requirements, hydrogel is a good option, which is permeable and tunable in many properties such as biodegradability, stiffness, adhesiveness and bioactivity.[40,41] However, because most hydrogels are soft and floppy, it remains a challenge to fabricate robust topographical features out of hydrogels in the length scales sufficient to impose topological cues to tune cell response. It is even more challenging to fabricate hydrogel scaffold with uniform micrometer topography across centimeter or even larger sizes.[42−46] The topic is sufficiently broad and important that ample room exists for exploring new materials, fine structures, and various types of cells for different applications.

In this research, we fabricate HEMA hydrogel substrates with high-aspect-ratio topographical features. The pHEMA hydrogel is chosen because of its good mechanical integrity[47,48] and biocompatibility.[49,50] We show that human mesenchymal stem cells (HMSCs) cultured on the microstructured hydrogel substrate can orient based on the underlying geometrical cues. Instead of rounding up as on the flat pHEMA hydrogel, the cells elongate and adhere on the patterned hydrogel substrate. The elongation and alignment of cell bodies are highly uniform. The effect of feature dimensions on the cell morphology and adhesion is also discussed. Such hydrogel substrates are shown to be viable for long-term cell culture and capable of generating interconnected cell monolayers with uniform orientation spanning centimeter sizes.

2. RESULTS AND DISCUSSION

The hydrogel substrates were made of poly(2-hydroxyethyl methacrylate) (pHEMA) monomer, ethylene glycol dimethyl acrylate (EGDMA) cross-linker, and 2-hydroxy-2-methyl-1-phenyl-propan-1-one (Darocur 1173) photoinitiator. The molecular structures of the chemicals are shown in Figure S1. The monomer to cross-linker ratio was 100:1. The linear swelling ratio of such fabricated pHEMA hydrogel in DI water was 1.4 ± 0.2, and the shear modulus of the swollen gel was 500 ± 100 kPa. It is much softer than most of the soft elastomers widely used for fabricating structured surfaces, e.g. polydimethylsiloxane, which has a shear modulus of 2 MPa.[51] The permeability of pHEMA gel was reported in the range of $7-9 \times 10^{-17}$ m^2.[52] It is higher than the widely used hydrogels for cell culture, e.g. polyacrylamide gel, which has a typical permeability of $4-5 \times 10^{-18}$ m^2.[53]

The microstructured hydrogel surface was fabricated through a two-step replica molding process. The procedure is illustrated in Figure 1a. Silicon masters with microplate arrays were fabricated by reactive ion etching (Figure 1b). The surfaces of the silicon masters were treated by oxygen plasma, followed by silanization to ensure easy detachment. A negative mold was

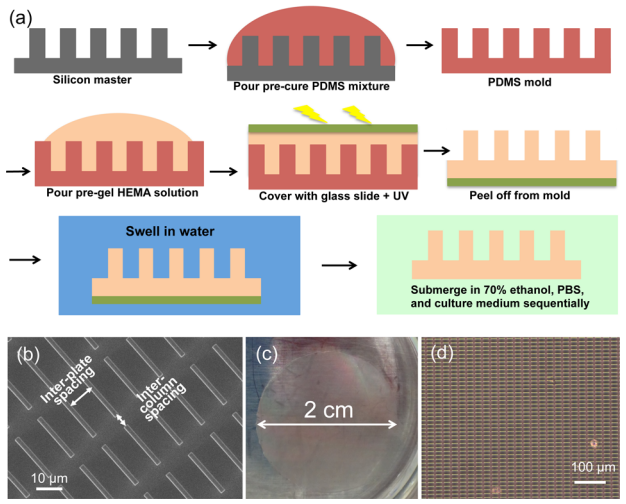

Figure 1. (a) Schematic illustration of the procedure for the fabrication of the microstructured hydrogel substrate. (b) Scanning electron microscopic image of the microplate arrays on the surface of the silicon master. (c) Picture of the hydrogel substrate. (d) Microscopic image of the hydrogel surface with microplate arrays duplicated from the silicon master.

fabricated using Polydimethylsiloxane (PDMS) elastomers. A drop of premixed hydrogel precursor was put on the PDMS mold, covered with a glass coverslip and cured by exposure to UV light. After curing, the hydrogel layer attached to the glass substrate through hydrogen bonding due to the existing hydroxyl groups, which allowed the hydrogel layer and the glass coverslip to be peeled off together from the PDMS mold. The sample was then submerged in water overnight, allowing the hydrogel layer to swell. Because of swelling, the hydrogel layer detached from the glass coverslip. Before the freestanding hydrogel film was used as cell culture substrate, it had been sterilized with ethanol solution and then saturated with cell culture medium. The diameter of the circular hydrogel film was around 2 cm and its thickness was ranging from 500 μm to 1 mm. As shown in Figure 1c, the film was transparent, showing iridescent color due to the regular structures on the surface. A representative microscopic image of the surface patterns is shown in Figure 1d. The plate arrays are highly regular with very few defects. The features from the original silicon master are well preserved. The regularity spans the whole sample surface. The dimensions of the hydrogel micro plates, as shown in Figure 1, are 2 μm in thickness, 20 μm in height, and 20 μm in width. The interplate spacing is 10 μm and the intercolumn spacing is 5 μm. The height-to-thickness ratio of the micro plates is 10. To the best of the authors' knowledge, making such small and high-aspect-ratio surface features on hydrogels over large surface areas has not been achieved before.

To systematically study the geometric effect on cell behavior, we designed and fabricated six modes of plate patterns. The dimensions of the patterns are summarized in Table 1. The hydrogel was fluorescently labeled and confocal images were taken from each pattern of the surface. To illustrate the three-dimensional configurations and dimensions of the surface patterns, orthogonal views of the confocal images are shown in Figure 2. The microplates tapered off from the bottom to the top and the sharp edges present in the original silicon masters were rounded in the duplicated hydrogel samples. Nevertheless, the dimension and geometry of the surface features from the original silicon masters were well-preserved.

DOI: 10.1021/acsami.5b12268
ACS Appl. Mater. Interfaces 2016, 8, 21939−21945

Table 1. Dimensions of the Six Modes of the Microplate Patterned Hydrogel Substrates

	I	II	III	IV	V	VI
plate width (μm)	10	25	50	10	25	50
plate height (μm)	18	18	18	18	18	18
plate thickness (μm)	2	2	2	2	2	2
interplate spacing (μm)	10	10	10	5	5	5
intercolumn spacing (μm)	5	5	5	5	5	5

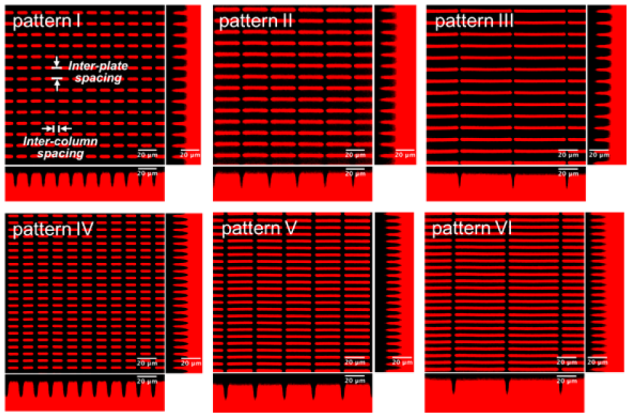

Figure 2. Orthogonal views of the confocal images of the pHEMA hydrogel substrates with six different patterns. The scale bar is 20 μm.

We first examined the viability of the pHEMA hydrogel for cell culture and the effect of the surface structures on cell attachment. For comparison, three different substrates were tested: regular cell culture Petri-dish, flat pHEMA hydrogel film, and microstructured pHEMA hydrogel film. The same batch of the HMSCs was seeded on the three substrates simultaneously and cultured in the same incubator under 37 °C and 4% CO_2. After 24 h, the cells showed distinct behaviors on the three substrates, as shown in Figure 3. Cells on a regular cell culture Petri-dish adhered and spread into multipolarized shapes, which is a common observation for HMSCs. Cells on a flat pHEMA hydrogel substrate did not spread. Instead, they rested on the substrate with a round shape, and were easily sheared off from the substrate. This behavior was observed before and was understood as being due to the hydrophilic surface property of the pHEMA hydrogels and the lack of anchor point on the flat surface.[54,55] However, on the same pHEMA hydrogel when it was fabricated with microstructures, HMSCs can adhere to it. The cells spread into specific elongated geometries in response to the topographical cues and fit into the interplate spaces (Figure 4a, b). A confocal image shows the spatial position of an attached cell in relation to the

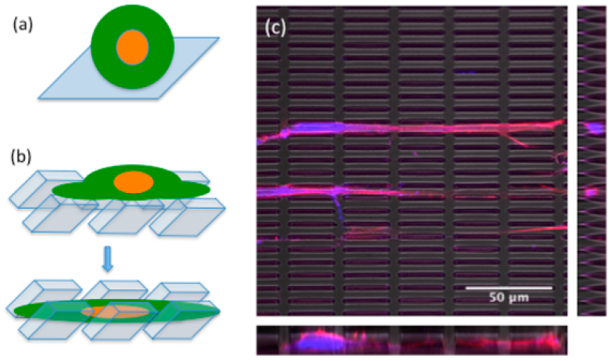

Figure 4. (a) Schematic illustration of the morphology of HMSCs on flat pHEMA hydrogels. (b) Schematic illustration of how a cell senses and responds to structural pHEMA surface. (c) Orthogonal views of a confocal image of the HMSCs attached and aligned on the microstructured pHEMA hydrogel surface confirm that the cells grow in between parallel plates.

microplates (Figure 4c). The actin filaments and the nuclei of the cells were fluorescently labeled. It shows the cell stays in between the parallel plates and conforms to the gap.

We studied the geometric effects further by fabricating six plate-patterned surfaces with different dimensions. For all the patterns, the thickness and height of the plates were 2 and 18 μm. From experience, when the plate thickness is smaller than 2 μm or its height is larger than 20 μm, the plates are prone to collapse. The width of the plate varied from 10, 25 to 50 μm. The interplate spacing varied between 5 to 10 μm in this study. When the interplate spacing was larger than 20 μm, the cells rounded up in between the plates as on the flat hydrogel substrate. In contrast, when the interplate spacing was less than 3 μm, the cells did not spread but stayed on top of the plates. With these constraints, six modes of plate patterns were fabricated (Figure 2 and Table 1). To rule out other factors that may influence the cell behaviors, the cells seeded on the six different substrates were always from the same batch. In each set of experiment, 12 hydrogel samples were prepared, two for each pattern. Each set of experiment was repeated three times. After 24 h in incubator, the cells on the hydrogel substrate were fixed with paraformaldehyde solution and fluorescently labeled with phalloidin for actin filaments, and DAPI (4′,6-diamidino-2-phenylindole) for nuclei, respectively. On each sample, 40–60 images were taken at different locations. Several typical

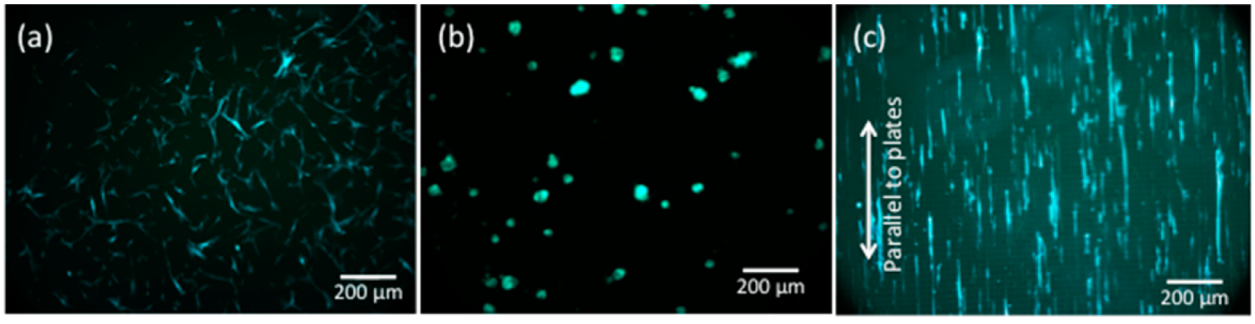

Figure 3. After 24 h of culture, HMSCs (a) adhere and spread on tissue culture Petri-dish, (b) round up on flat pHEMA hydrogel substrate, and (c) elongate and align on microplate patterned pHEMA hydrogel substrate.

DOI: 10.1021/acsami.5b12268
ACS Appl. Mater. Interfaces 2016, 8, 21939–21945

images of the cell morphologies on each pattern are shown in Figure 5a.

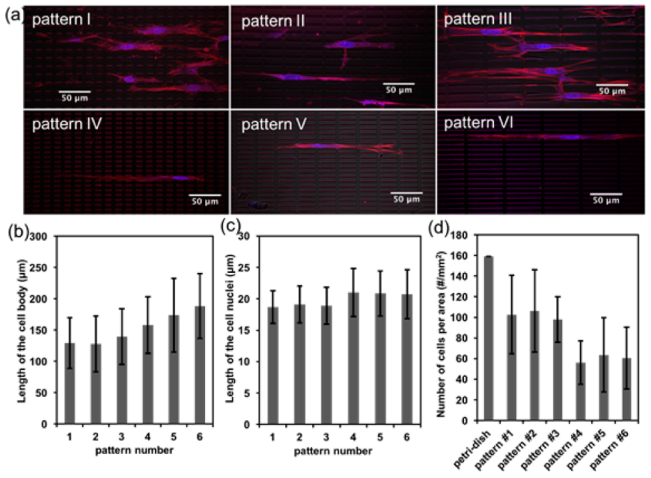

Figure 5. (a) Representative pictures of HMSCs on the microstructured hydrogel surface. (b) Quantitative measurements of the cell length on the six different patterns. (c) Quantitative measurements of length of the cell nuclei on the six patterns. (d) The average number of cells adhering to the Petri-dish and different patterned hydrogel surfaces.

The six patterns allow us to study the effect of two factors that influence the cell shape: the size of the interplate spacing and the width of the plate. We first quantified the lengths of the cell body on each pattern through image analysis (Figure 5b). We observed that the elongation of the cell body is sensitive to the size of the interplate spacing. The cells on patterns I, II and III, which have a wider interplate spacing of 10 μm, elongated less than those grown on patterns IV, V, and VI, which have a narrower interplate spacing of 5 μm. To quantify this effect, we compared the two patterns that have the same plate width but different interplate spacing, i.e. pattern I vs IV, II vs V, and III vs VI, and calculated the relative increase of the cell length. For instance, we denote the average cell length on pattern-I as l_I, and the average cell length on pattern-IV as l_{IV}. We then calculate the relative increase as $(l_I - l_{IV})/ l_I$. Consequently, we obtained a 22.5% increase of cell length on pattern IV compared with pattern I, a 35.1% increase on pattern V compared with pattern II, and a 35.3% increase on pattern VI compared with pattern III. To fit into a smaller space between the parallel plates, the cells need to squeeze themselves more in the lateral direction, and they do so by stretching more in the longitudinal direction. From Figure 5b, we also observe that the elongation of the cell body is slightly sensitive to the plate width. On wider plates, the cells tend to elongate more. For instance, the patterns IV, V, and VI have the same interplate spacing of 5 μm, but different plate width. From IV to VI, the plate width increases sequentially from 10 μm, 20 to 50 μm, and the length of the cells grown on these patterns increases accordingly. The same trend is also shown on patterns I to III, but less significant. When the plates are wide, the cells have less probability to branch out in the lateral direction through the intercolumn spacing, and thus the growth is mostly confined in the longitudinal direction. We also quantified the lengths of the cell nuclei on each pattern of the substrate through image analysis and the results are shown in Figure 5c. We observed that on narrower interplate spaces, i.e., patterns IV, V, and VI, the length of the cell nuclei is longer. We did not observe statistically significant dependence of nuclei length on the plate width. We further quantified the average number of cells adhering on the patterned substrate. As shown in Figure 5d, comparing with cell culture Petri-dish, less cells adhere to the patterned substrate, and the narrower the interplate spacing is, the fewer cells adhere to the substrate due to the geometric confinement. Considering cells as wetting liquid,[56] surface energy decreases as they fit into the structures, while considering cells as soft solid,[57] the elastic energy increases as they stretch longer. As shown in Figure 6a, b, the surface energy

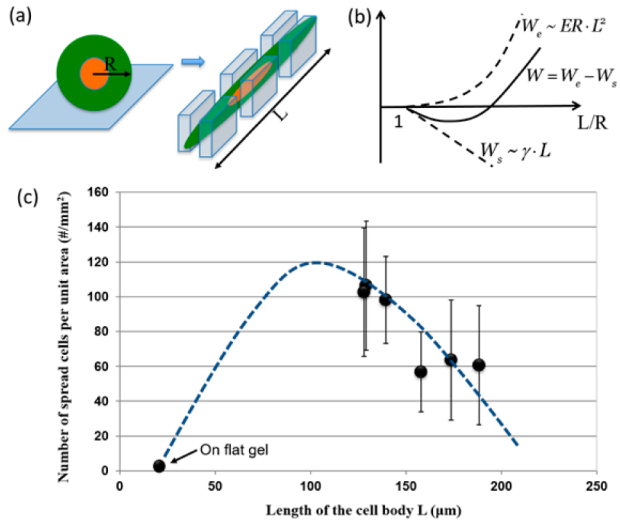

Figure 6. (a) Cells round up on the flat gel surface but elongate and adhere to the plate-patterned gel. (b) Schematic of the growth mechanism: the surface energy decreases linearly as cell length; elastic energy increases quadratically as cell length; and the overall energy decreases first and then increases as cell length. (c) After 24 h of culture, the number of cells adhering to different patterned hydrogels is plotted against cell length.

decreases linearly as cell length, while the elastic energy increases quadratically as cell length. The overall energy decreases and then increases. Correspondingly in experiment, we observed that the number of spreading cells per unit area increases and then decreases as the cell length (Figure 6c). Comparing with flat hydrogel substrate, the patterned substrates provide more available surfaces, and it is energetically favorable for the cells to elongate to fit in, but as the interplate space becomes narrower, although it provides more effective surface per unit projected area, the elastic energy that the cells have to overcome in order to fit in becomes predominant, and it is energetically less favorable for the cells to fit in.

The microstructured pHEMA hydrogel substrates are viable for long-term cell culture. As shown in Figure 7a and Figure S2, the cells on the hydrogel substrate grow into a dense and interconnected layer. The connection in vertical direction is through the intercolumn spacing. As shown in the confocal image of Figure 7b. This is one of the advantages of having plate-patterned substrate over groove-patterned substrate, which is the conventional design of patterned substrate, to induce cell bipolarization. We also quantified the growth of cells on the patterned substrate through cell viablity assay. The cell proliferation rates on the culture Petri-dish and on the microstructured hydrogels were recorded and shown in Figure S3 and Figure 8, respectively. The proliferation rate on the

DOI: 10.1021/acsami.5b12268
ACS Appl. Mater. Interfaces 2016, 8, 21939−21945

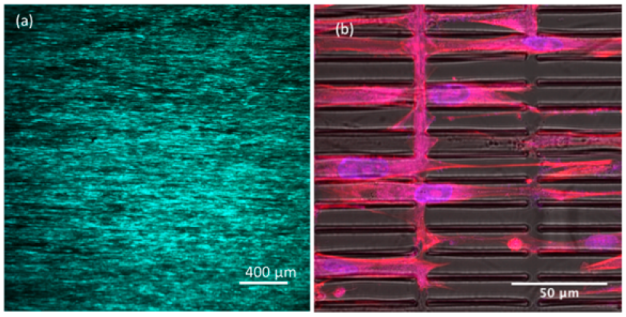

Figure 7. (a) After 32 days of culture, the cells on the microstructured hydrogel substrate grow into a dense and interconnected layer. (b) A confocal image shows that the cells connect through the intercolumn spaces. The picture was taken after 7 days of culture.

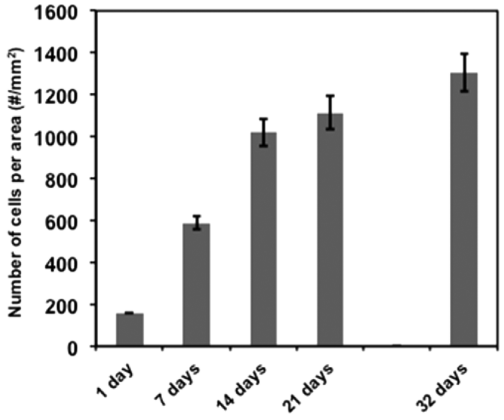

Figure 8. Viability of long-time culture on the gel substrates. The average number of cells per unit projected area is plotted against in culture.

microstructured hydrogel is slower than on Petri-dish surface. It might be due to the geometric confinement of the structures. Nonetheless, the HMSCs cultured on the patterned hydrogel substrate retain the ability to divide even after one month (Figure 8).

3. CONCLUSIONS

On one hand, micro/nanostructured surfaces have been shown to be a promising tool to realize cell guidance. The topological cues can direct cell morphology and induce stem cell differentiation. On the other hand, hydrogels have been extensively studied as the most promising media to mimic the extracellular environment of human bodies. Putting the two ingredients together, hydrogel and surface topography, can potentially create a new avenue for cellular and tissue engineering. In this study, we showed that high-aspect-ratio microfeatures can be fabricated out of hydrogels. The structured hydrogel surface could effectively direct cell shape and control cell adhesion. The influence of the dimensions of the surface structures on cell morphology was carefully studied. The permeable nature of hydrogels makes them an ideal media for long-term culture. The hydrogel can be molded into any shape, and its chemical and physical properties can be easily tailored. For instance, to broaden its biomedical application, we can easily introduce the biodegradability into the pHEMA gels.[50] This study provides a stepping-stone for the future design of soft scaffolds that can fine-tune the cell morphology and at the same time produce three-dimensional foldable shapes that better mimic the extracellular environment, providing solutions for easy transplantation.

4. EXPERIMENTAL SECTION

Materials. The chemicals for making pHEMA gel include the monomer 2-hydroxyethyl methacrylate (HEMA), the cross-linker ethylene glycol dimethyl acrylate (EGDMA), and the photoinitiator 2-hydroxy-2-methyl-1-phenyl-propan-1-one (Darocur 1173). They were purchased from Sigma-Aldrich (Atlanta, GA). Their chemical structures are shown in Figure 1S. The Polydimethylsiloxane (PDMS) precursor and curing agent (Sylgard 184) were obtained from Dow Corning. The chemicals used for cell culture and fluorescent labeling including the alpha-MEM media, the penicillin-Streptomycin (Pen Strep), the fetal bovine serum (FBS), the phosphate buffered saline (PBS) buffer, the trypsin-EDTA, the 4′,6-diamidino-2-phenylindole (DAPI), the Alexa Fluor 594 Phalloidin, and the 5-chloromethylfluorescein diacetate (CellTracker Green) were purchased from Life Technologies Corporation (Chicago, IL). Paraformaldehyde for fixation of cells was purchased from VWR International Inc. (Pittsburgh, PA). All of the chemicals were used without further purification.

pHEMA Hydrogel Substrate. The hydrogel substrates with microplate-array topography were fabricated by using a two-step replica molding process (Figure 1a). Silicon microplate arrays were fabricated by deep UV stepper lithography and Bosch deep reactive ion etching (DRIE) of single-crystal silicon wafers. The surfaces of the silicon masters were treated by oxygen plasma, and hydrophobic samples were prepared by silanization with (tridecafluoro-1,1,2,2-tetrahydrooctyl) trichlorosilane (Gelest, Inc. Morrisville, PA, USA). Liquid PDMS precursor in a 10:1 (base: curing agent) ratio was poured onto the silicon master and cured at 70 °C for 2 h. The cured PDMS was peeled off from the master. The negative PDMS mold contained an array of high-aspect-ratio wells corresponding to the plates of the positive master. The gel precursor solution was prepared by mixing 2.5 mL of HEMA with 75 μL of Darocur 1173. The mixture was exposed to UV light with the power of 16 mW/cm^2 for 60 s. Before molding, an additional 50 μL of Darocur 1173 and 25 μL of EGDMA were added to this solution and stirred overnight. To fabricate the hydrogel microplate arrays, the gel solution was poured on the PDMS mold, covered by a circular glass coverslip of 18 mm diameter, and exposed to UV light with the power of 130 mW/cm^2 for 60 s. The gel substrate together with the glass coverslip was gently peeled off from the PDMS mode. The structure was then submerged in water overnight. The hydrogel swelled and detached from the glass slide. The freestanding gel substrate was washed with 10, 30, 50, 70, 50, 30, and 10% ethanol solutions in sequence. Before use, the gel substrate was washed with PBS three times and submerged in cell culture medium for 2h.

Mechanical Characterization of pHEMA Hydrogels. For material characterization, bulk hydrogel samples were fabricated. The diameter and thickness of the sample were measured before and after swelling in DI water. The swelling ratio was calculated as the linear dimension of the gel in swollen state divided by that in dry state. Three samples were fabricated and tested. The three samples were further tested under compression measurements. The samples were under DI water during testing. The loading rate was 0.1 mm/s and the maximum displacement applied was 1 mm. The force was recorded as the sample was compressed. A linear stress−strain relation was assumed and the Young's modulus was calculated accordingly. Shear modulus was calculated with a Poisson's ratio of 0.5.

HMSC Cell Culture and Observation. Human adult mesenchymal stem cells were obtained from Texas A&M Health Science Center College of Medicine. Cells were cultured in alpha-MEM supplemented with L-glutamate (2 mM), penicillin (100 U/mL), and streptomycin containing 16.5% heat-inactivated FBS. Cells were expanded in T75 flask and subcultured prior to confluence. All the cells were used at passages between 6 and 8. Cells were seeded on the gel substrate at concentration of 80 cells/cm^2 and cultured. After 24 h in culture, the cells on the hydrogel substrate were rinsed in serum free

DOI: 10.1021/acsami.5b12268
ACS Appl. Mater. Interfaces 2016, 8, 21939−21945

media and fixed with 4% paraformaldehyde in 0.1 M PBS for 30 min. The cells were then stained with phalloidin (Alexa-Fluor 594), DAPI and cell tracker green according to the manufacturer's instructions to visualize filamentous F-actin, cell nuclei, and the whole cell body, respectively. Visualization was made with an inverted microscope (Zeiss Axiovert 40CFL 3) and a confocal microscope (Upright Zeiss LSM 710).

Cell Viability Assay. CellTiter-Glo Luminescent Cell Viability Assay was purchased from Promega corporation. Before use, we thawed the CellTiter-Glo buffer and CellTiter-Glo substrate to room temperature, and mixed 1 vial of the substrate with 10 mL buffer for 2 min by gently vortexing the mixture. We diluted the mixture with cell culture buffer at 1:1 ratio, covered the hydrogel sample with 3 mL of the diluted reagent and allowed for 15 min incubation at room temperature. We then transferred the reactive solution into opaque 96-well plates with 100 μL per well and the luminescent signals were recorded by a Spectramax L Plate Reader (Molecular Devices Corp., Sunnyvale, CA, USA).

■ ASSOCIATED CONTENT

Supporting Information

The Supporting Information is available free of charge on the ACS Publications website at DOI: 10.1021/acsami.5b12268.

Figures S1−S3 (PDF)

■ AUTHOR INFORMATION

Corresponding Author

*E-mail: yuhanghu@illinois.edu.

Funding

NSF Materials Research Science and Engineering Center (MRSEC) at Harvard University under Award DMR 14−20570

Notes

The authors declare no competing financial interest.

■ ACKNOWLEDGMENTS

This work was supported by the NSF Materials Research Science and Engineering Center (MRSEC) at Harvard University under Award DMR 14-20570. Y.H. thanks Dr. Yolanda Vasquez for teaching her the basics about cell culture.

■ REFERENCES

(1) Papadaki, M.; Bursac, N.; Langer, R.; Merok, J.; Vunjak-Novakovic, G.; Freed, L. E. Tissue Engineering of Functional Cardiac Muscle: Molecular, Structural, and Electrophysiological Studies. *Am. J. Physiol. Heart Circ. Physiol.* **2001**, *280*, H168−H178.

(2) Wigmore, P. M.; Dunglison, G. F. The Generation of Fiber Diversity during Myogenesis. *Int. J. Dev. Biol.* **1998**, *42*, 117−125.

(3) Chiu, J. J.; Chen, L. J.; Chen, C. N.; Lee, P. L.; Lee, C. I. A Model for Studying the Effect of Shear Stress on Interactions between Vascular Endothelial Cells and Smooth Muscle Cells. *J. Biomech.* **2004**, *37*, 531−539.

(4) Vunjak-Novakovic, G.; Altman, G.; Horan, R.; Kaplan, D. L. Tissue Engineering of Ligaments. *Annu. Rev. Biomed. Eng.* **2004**, *6*, 131−156.

(5) Ghosh, K.; Ingber, D. E. Micromechanical Control of Cell and Tissue Development: Implications for Tissue Engineering. *Adv. Drug Delivery Rev.* **2007**, *59*, 1306−1318.

(6) Langer, R.; Vacanti, J. P. Tissue Engineering. *Science* **1993**, *260*, 920−926.

(7) Griffith, L. G.; Naughton, G. Tissue Engineering—Current Challenges and Expanding Opportunities. *Science* **2002**, *295*, 1009−1014.

(8) Whitesides, G. M.; Ostuni, E.; Takayama, S.; Jiang, X.; Ingber, D. E. Soft Lithography in Biology and Biochemistry. *Annu. Rev. Biomed. Eng.* **2001**, *3*, 335−373.

(9) Kane, R. S.; Takayama, S.; Ostuni, E.; Ingber, D. E.; Whitesides, G. M. Patterning Proteins and Cells Using Soft Lithography. *Biomaterials* **1999**, *20*, 161−174.

(10) Chen, C. S.; Jiang, X. Y.; Whitesides, G. M. Microengineering the Environment of Mammalian Cells in Culture. *MRS Bull.* **2005**, *30*, 194−201.

(11) McBeath, R.; Pirone, D. M.; Nelson, C. M.; Bhadriraju, K.; Chen, C. S. Cell Shape, Cytoskeletal Tension, and RhoA Regulate Stem Cell Lineage Commitment. *Dev. Cell* **2004**, *6*, 483−495.

(12) Guck, J.; Lautenschlager, F.; Paschke, S.; Beil, M. Critical Review: Cellular Mechanobiology and Amoeboid Migration. *Integr. Biol.* **2010**, *2*, 575−583.

(13) Thery, M. Micropatterning As A Tool to Decipher Cell Morphogenesis and Functions. *J. Cell Sci.* **2010**, *123*, 4201−4213.

(14) Folch, A.; Toner, M. Microengineering of Cellular Interactions. *Annu. Rev. Biomed. Eng.* **2000**, *2*, 227−256.

(15) Singhvi, R.; Kumar, A.; Lopez, G. P.; Stephanopoulos, G. N.; Wang, D. I. C.; Whitesides, G. M.; Ingber, D. E. Engineering Cell Shape and Function. *Science* **1994**, *264*, 696−698.

(16) Ingber, D. E. Mechanical Control of Tissue Morphogenesis during Embryological Development. *Int. J. Dev. Biol.* **2006**, *50*, 255−266.

(17) Jiang, X.; Bruzewicz, D. A.; Wong, A. P.; Piel, M.; Whitesides, G. M. Directing Cell Migration with Ssymmetric Micropatterns. *Proc. Natl. Acad. Sci. U. S. A.* **2005**, *102*, 975−978.

(18) Doyle, A. D.; Wang, F. W.; Matsumoto, K.; Yamada, K. M. One-dimensional Topography Underlies Three-dimensional Fibrillar Cell Migration. *J. Cell Biol.* **2009**, *184*, 481−490.

(19) Kilian, K. A.; Bugarija, B.; Lahn, B. T.; Mrksich, M. Geometric Cues for Directing the Differentiation of Mesenchymal Stem Cells. *Proc. Natl. Acad. Sci. U. S. A.* **2010**, *107*, 4872−4877.

(20) Chen, C. S.; Mrksich, M.; Huang, S.; Whitesides, G. M.; Ingber, D. E. Geometric Control of Cell Life and Death. *Science* **1997**, *276*, 1425−1428.

(21) Nikkhah, M.; Edalat, F.; Manoucheri, S.; Khademhosseini, A. Engineering Microscale Topographies to Control the Cell-substrate Interface. *Biomaterials* **2012**, *33*, 5230−5246.

(22) Rorth, P. Whence Directionality: Guidance Mechanisms in Solitary and Collective Cell Migration. *Dev. Cell* **2011**, *20*, 9−18.

(23) Franco, D.; Klingauf, M.; Bednarzik, M.; Cecchini, M.; Kurtcuoglu, V.; Gobrecht, J.; Poulikakos, D.; Ferrari, A. Control of Initial Endothelial Spreading by Topographic Activation of Focal Adhesion Kinase. *Soft Matter* **2011**, *7*, 7313−7324.

(24) Charest, J. L.; Garcia, A. J.; King, W. P. Myoblast Alignment and Differentiation on Cell Culture Substrates with Microscale Topography and Model Chemistries. *Biomaterials* **2007**, *28*, 2202−2210.

(25) Oakley, C.; Jaeger, N. A. F.; Brunette, D. M. Sensitivity of Fibroblasts and Their Cytoskeletons to Substratum Topographies: Topographic Guidance and Topographic Compensation on Micromachined Grooves of Different Dimensions. *Exp. Cell Res.* **1997**, *234*, 413−424.

(26) Walboomers, X. F.; Croes, H. J. E.; Ginsel, L. A.; Jansen, J. A. Contact Guidance of Rat Fibroblasts on Various Implant Materials. *J. Biomed. Mater. Res.* **1999**, *47*, 204−212.

(27) Biela, S. A.; Su, Y.; Spatz, J. P.; Kemkemer, R. Different Sensitivity of Human Endothelial Cells, Smooth Muscle Cells and Fibroblasts to Topography in the Nano-Micro Range. *Acta Biomater.* **2009**, *5*, 2460−2466.

(28) Lu, J.; Rao, M. P.; MacDonald, N. C.; Khang, D.; Webster, T. J. Improved Endothelial Cell Adhesion and Proliferation on Patterned Titanium Surfaces with Rationally Designed, Micrometer to Nanometer Features. *Acta Biomater.* **2008**, *4*, 192−201.

(29) Bettinger, C. J.; Orrick, B.; Misra, A.; Langer, R.; Borenstein, J. T. Microfabrication of Poly (glycerol-sebacate) for Contact Guidance Applications. *Biomaterials* **2006**, *27*, 2558−2565.

(30) Yim, E. K. F.; Reano, R. M.; Pang, S. W.; Yee, A. F.; Chen, C. S.; Leong, K. W. Nanopattern-induced Changes in Morphology and Motility of Smooth Muscle Cells. *Biomaterials* **2005**, *26*, 5405−5413.

DOI: 10.1021/acsami.5b12268
ACS Appl. Mater. Interfaces 2016, 8, 21939−21945

(31) Karuri, N. W.; Liliensiek, S.; Teixeira, A. I.; Abrams, G.; Campbell, S.; Nealey, P. F.; Murphy, C. J. Biological Length Scale Topography Enhances Cell-substratum Adhesion of Human Corneal Epithelial Cells. *J. Cell Sci.* **2004**, *117*, 3153−3164.
(32) Rajnicek, A. M.; Foubister, L. E.; McCaig, C. D. Prioritising Guidance Cues: Directional Migration Induced by Substratum Contours and Electrical Gradients is Controlled by A Rho/cdc42 Switch. *Dev. Biol.* **2007**, *312*, 448−460.
(33) Lu, X.; Leng, Y. Comparison of the Osteoblast and Myoblast Behavior on Hydroxyapatite Microgrooves. *J. Biomed. Mater. Res., Part B* **2009**, *90B*, 438−445.
(34) Yim, E. K. F.; Pang, S. W.; Leong, K. W. Synthetic Nanostructures Inducing Differentiation of Human Mesenchymal Stem Cells into Neuronal Lineage. *Exp. Cell Res.* **2007**, *313*, 1820−1829.
(35) Rajnicek, A.; Britland, S.; McCaig, C. Guidance of CNS Growth Cones by Substratum Grooves and Ridges: Effects of Inhibitors of the Cytoskeleton, Calcium Channels and Signal Transduction Pathways. *J. Cell Sci.* **1997**, *110*, 2915−2924.
(36) Clark, P.; Connolly, P.; Curtis, A. S. G.; Dow, J. A. T.; Wilkinson, C. D. W. Topographical Control of Cell Behaviour: II. Multiple Grooved Substrata. *Development* **1990**, *108*, 635−644.
(37) Li, J. M.; McNally, H.; Shi, R. Enhanced Neurite Alignment on Micro-patterned Poly-L-lactic Acid Films. *J. Biomed. Mater. Res., Part A* **2008**, *87A*, 392−404.
(38) Bettinger, C. J.; Zhang, Z.; Gerecht, S.; Borenstein, J. T.; Langer, R. Enhancement of in Vitro Capillary Tube Formation by Substrate Nanotopography. *Adv. Mater.* **2008**, *20*, 99−103.
(39) Bettinger, C. J.; Bruggeman, J. P.; Borenstein, J. T.; Langer, R. S. Amino Alcohol-based Degradable Poly(ester amide) Elastomers. *Biomaterials* **2008**, *29*, 2315−2325.
(40) Hoffman, A. S. Hydrogels for Biomedical Applications. *Adv. Drug Delivery Rev.* **2002**, *54*, 3−12.
(41) Seliktar, D. Designing Cell-Compatible Hydrogels for Biomedical Applications. *Science* **2012**, *336*, 1124−1128.
(42) Park, H. S.; Lee, S. Y.; Yoon, H.; Noh, I. Biological Evolution of Micro-patterned Hyaluronic Acid Hydrogel for Bone Tissue Engineering. *Pure Appl. Chem.* **2014**, *86*, 1911−1922.
(43) Koh, W.-G.; Itle, L.; Pishko, M. V. Molding of Hydrogel Microstructures to Create Multiphenotype Cell Microarrays. *Anal. Chem.* **2003**, *75*, 5783−5789.
(44) Lutolf, M. P.; Doyonnas, R.; Havenstrite, K.; Koleckar, K.; Blau, H. M. Perturbation of Single Hematopoietic Stem Cell Fates in Artificial Niches. *Integr. Biol.* **2009**, *1*, 59−69.
(45) Khetan, S.; Burdick, J. A. Patterning Network Structure to Spacially Control Cellular Remodeling and Stem Cel Fate within 3-dimensional Hydrogels. *Biomaterials* **2010**, *31*, 8228−8234.
(46) Segura, T.; Anderson, B. C.; Chung, P. H.; Webber, R. E.; Shull, K. R.; Shea, L. D. Crosslinked Hyaluranic Acid Hydrogels: A Strategy to Functionalize and Pattern. *Biomaterials* **2005**, *26*, 359−371.
(47) Chandra, D.; Yang, S.; Soshinsky, A. A.; Gambogi, R. J. Biomimetic Ultrathin Whitening by Capillary-force-induced Random Clustering of Hydrogel Micropillar Arrays. *ACS Appl. Mater. Interfaces* **2009**, *1*, 1698−1704.
(48) You, J.-O.; Auguste, D. T. Nanocarrier Cross-linking Density and pH Sensitivity Regulate Intracellular Gene Transfer. *Nano Lett.* **2009**, *9*, 4467−4473.
(49) Abraham, S.; Brahim, S.; Ishihara, K.; Guiseppi-Elie, A. Molecularly Engineered p(HEMA)-based Hydrogels for Implant Biochip Biocompatibility. *Biomaterials* **2005**, *26*, 4767−4778.
(50) Zhang, Y.; Chu, D.; Zheng, M.; Kissel, T.; Agarwal, S. Biocompatible and Degradable poly(2-hydroxyethylmethacrylate) Based Polymers for Biomedical Applications. *Polym. Chem.* **2012**, *3*, 2752−2759.
(51) Hu, Y.; Chen, X.; Whitesides, G. M.; Vlassak, J. J.; Suo, Z. Indentation of Polydimethylsiloxane Submerged in Organic Solvents. *J. Mater. Res.* **2011**, *26*, 785−795.
(52) Refojo, M. F. Permeation of Water Through Some Hydrogels. *J. Appl. Polym. Sci.* **1965**, *9*, 3417−3426.
(53) Kalcioglu, Z. I.; Mahmoodian, R.; Hu, Y.; Suo, Z.; Van Vliet, K. J. From Macro- to Microscale Poroelastic Characterization of Polymeric Hydrogles via Indentation. *Soft Matter* **2012**, *8*, 3393−3398.
(54) Folkman, J.; Moscona, A. Role of Cell Shape in Growth Control. *Nature* **1978**, *273*, 345−349.
(55) Deligianni, D. D.; Katsala, N. D.; Koutsoukos, P. G.; Missirlis, Y. F. Effect of Surface Roughness of Hydroxyapatite on Human Bone Marrow Cell Adhesion, Proliferation, Sifferentiation and Setachment Strength. *Biomaterials* **2000**, *22*, 87−96.
(56) Gonzalez-Rodriguez, D.; Guevorkian, K.; Douezan, S.; Brochard-Wyart, F. Soft Matter Models of Developing Tissues and Tumors. *Science* **2012**, *338*, 910−917.
(57) Kasza, K. E.; Rowat, A. C.; Liu, J.; Angelini, T. E.; Brangwynne, C. P.; Koenderink, G. H.; Weitz, D. A. The Cell as A Material. *Curr. Opin. Cell Biol.* **2007**, *19*, 101−107.

DOI: 10.1021/acsami.5b12268
ACS Appl. Mater. Interfaces 2016, 8, 21939−21945